Temperature-Controlled Growth of ZnO Nanowires and Nanoplates in the Temperature Range 250−300 °C

Congkang Xu,[†] Dongeon Kim,*[,†,‡] Junghwan Chun,[†] Keehan Rho,[†] Bonghwan Chon,[§] Sangsu Hong,[§] and Taiha Joo[§]

Physics Department and Electron Spin Science Center, Pohang University of Science and Technology, San 31, Hyoja-Dong, Namku, Kyungbuk 790-784, Republic of Korea, Nanodevice Research Center, Korea Institute of Science and Technology, P.O. Box 131, Chengryang, Seoul 130-650, Korea, and Department of Chemistry, Pohang University of Science and Technology, Pohang, 790-784, Republic of Korea

Received: May 23, 2006; In Final Form: July 20, 2006

Starting from a mixture of Zn and BiI_3, we grew nanowires and nanoplates on an oxidized Si substrate at relatively low temperatures of 250 and 300 °C, respectively. The ZnO nanowires had diameters of ∼40 nm and grew along the [11$\bar{2}$0] direction rather than the conventional [0001] direction. The nanoplates had thicknesses of ∼40 nm and lateral dimensions of 3−4 μm. The growth of both the nanowires and nanoplates is dominated by the synergy of vapor−liquid−solid (VLS) and direction conducting. Analysis of photoluminescence spectra suggested that the nanoplates contain more oxygen vacancies and have higher surface-to-volume ratios than the nanowires. The present results clearly demonstrate that the shapes of ZnO nanostructures formed by using BiI_3 can be controlled by varying the temperature in the range 250−300 °C.

1. Introduction

ZnO nanostructures have attracted considerable interest because of their diverse potential applications.[1−4] These ZnO nanostructures are usually fabricated under high temperatures (>400 °C). This high-temperature environment is not well suited to other processing techniques in nanodevice fabrication and integration.[5] Low-temperature fabrication is therefore desirable and important for nanodevices, especially those in which the substrate and nanostructures have different compositions. In addition to the potential applications of 1D nanostructures, 2D nanostructures can be directly utilized not only in the fabrication of devices but also as a transition stage in the formation of other nanostructures; for example, nanowalls formed from layer-structured carbon have been used as templates to deposit magnetic nanoparticles.[6] Wet chemistry and solid−vapor methods are currently the two main approaches used to synthesize 2D nanostructures. The thermolysis of various organometallic precursors in surfactant solutions has been successfully used to fabricate 2D nanostructures.[7−10] This approach is particularly intriguing because the selective absorption of the surfactant may control the size and shape of the nanostructure. Nonetheless, it is still difficult to grow nanostructures on the substrate in the solution. The usefulness of the vapor-phase transport (VPT) route is also limited by its low yields and need for high temperatures.[11] In terms of practical nanodevice applications, not only the ability to fabricate 1D or 2D nanostructures at low temperatures but also the ability to control the shapes of these nanostructures at low temperatures is desirable. Although several examples have been reported, shape control has proved difficult to achieve and remains a key challenge. It would be ideal if one could integrate VPT into the selective absorption of the surfactant at low temperature. One approach that could potentially facilitate control of the shape of ZnO nanostructures (i.e., nanowires and nanoplates) would be to use a precursor that can also form a low-melting-point alloy with Zn and have the function of selective absorption of the surfactant. Here, we consider ZnI_2 and BiI_3, both of which tend to sublime at low temperatures.[12] Moreover, Bi and Zn can form a Zn−Bi alloy with a low melting point, which can act as a catalyst for the low-temperature growth of 1D ZnO nanostructures. I^- and I_2 are highly polarizable, and both can interact with the polar ZnO surface, leading to the shape control of ZnO nanostructures.[13]

In this paper, we report the results of experiments carried out in a VPT furnace with a vacuum pumping system, using Zn and BiI_3 as starting materials, an oxidized silicon wafer as the substrate, and argon gas as the protective gas. We show that, by using the iodide, we could control the shape of the resulting ZnO nanostructures. Specifically, ZnO nanowires were formed at 250 °C and ZnO nanoplates were formed at 300 °C, with intermediate structures being observed at temperatures between 250 and 300 °C.

2. Method Section

The experimental setup used to grow the nanowires and nanoplates was the same as that in previous reports.[14,15] Briefly, bismuth iodide (99.999%, Aldrich) and zinc (99.998%, 100 mesh, Aldrich) were homogeneously mixed in a weight ratio of 1:3 using a mortar and pestle. The resulting mixture was loaded into an 8-cm-long alumina boat, which was then covered by three pieces of oxidized silicon substrate separated by gaps of approximately 1 mm. The covered boat was then placed in the center of a quartz tube. The base vacuum in the tube was about 300 m Torr. High-purity argon gas was fed into the tube at a flow rate of 150 sccm. The furnace was heated to 250 or 300 °C and held at that temperature for 30 min. The air was momentarily introduced into the reaction chamber through the

* Corresponding author. E-mail: kimd@postech.ac.kr.
[†] Physics Department and Electron Spin Science Center, Pohang University of Science and Technology.
[‡] Korea Institute of Science and Technology.
[§] Department of Chemistry, Pohang University of Science and Technology.

10.1021/jp0631681 CCC: $33.50
Published on Web 09/22/2006

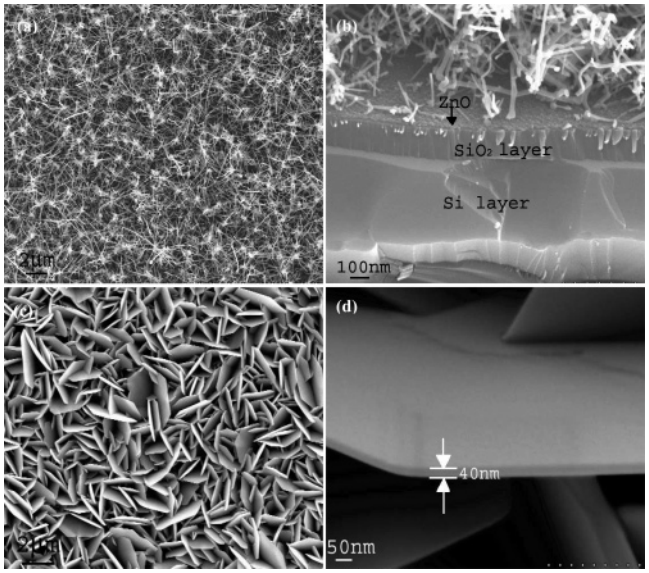

Figure 1. (a) SEM image of the ZnO nanowires grown on an oxidized Si substrate at 250 °C. (b) SEM tilted view of ZnO nanowires at 250 °C. (c) SEM image of the nanoplates grown on an oxidized Si substrate at 300 °C. (d) Magnified SEM image of a nanoplate at 300 °C.

outlet end of the furnace while maintaining the temperature. The furnace was then cooled to ambient temperature.

The morphologies of the products on the substrates were examined using a scanning electron microscope (SEM) equipped with an energy-dispersive X-ray spectrometry (EDX) system and a JEOL-2010 high-resolution transmission electron microscope (TEM) equipped with an energy-dispersive X-ray spectrometry (EDX) system and a Japanese Rigaku D/max γA X-ray powder diffractometer (XRD). Photoluminescence (PL) spectra were recorded at 10 and 300 K, using 300 nm and 355 nm lights as the excitation sources.

3. Results and Discussion

Figure 1 shows SEM images of the nanowires grown at 250 °C and nanoplates grown at 300 °C. As shown in Figure 1a, the nanowires grown at 250 °C are very dense and distributed over the entire substrate surface. The nanowires have an average diameter of about 40 nm and are each a few micrometers long. The tilted SEM image of the ZnO nanowires in Figure 1b clearly shows a thin layer (indicated by a black arrow) beneath the nanowires. The SEM images of the ZnO nanoplates grown at 300 °C (Figure 1c and d) show a high density of nanoplates distributed over the entire substrate surface. The magnified SEM image in Figure 1d shows that the nanoplates have lateral dimensions of 3−4 μm and a thickness of ~40 nm. It is clear from Figure 1 that the nanostructure generated by the proposed method can be varied from a nanowire to a nanoplate structure by a quite small temperature change in the low-temperature region. Moreover, Figure 1a and c indicates that both the nanowires and nanoplates were obtained in very high yield.

Figure 2 shows XRD patterns of the ZnO nanowires and nanoplates on oxidized Si substrates. The diffraction peaks of the ZnO nanowires (Figure 2a) are quite similar to those of bulk ZnO with a hexagonal wurtzite structure (a = 3.18 Å, c = 5.18 Å) and conventional ZnO nanowires grown at high temperatures.[4] No typical diffraction peaks corresponding to Bi or Bi compound impurity phases were observed. For the ZnO nanoplates (Figure 2b), the reflections from (100), (002), and (110) planes are weak, whereas those from (101), (102), and (103) planes are quite strong, unlike the conventional nanodisks, in

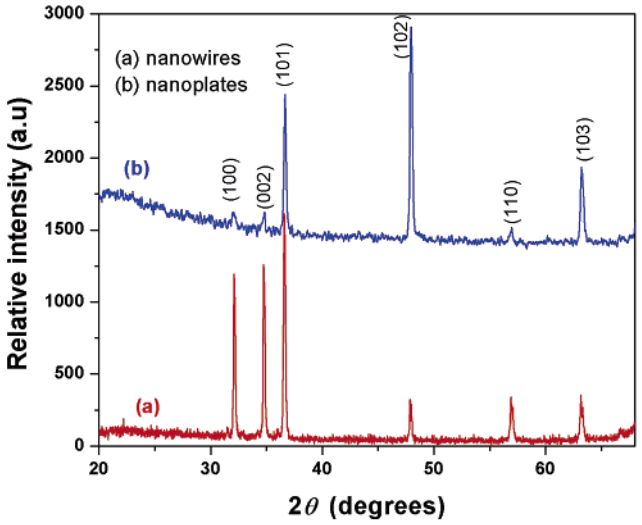

Figure 2. XRD patterns of (a) ZnO nanowires and (b) ZnO nanoplates.

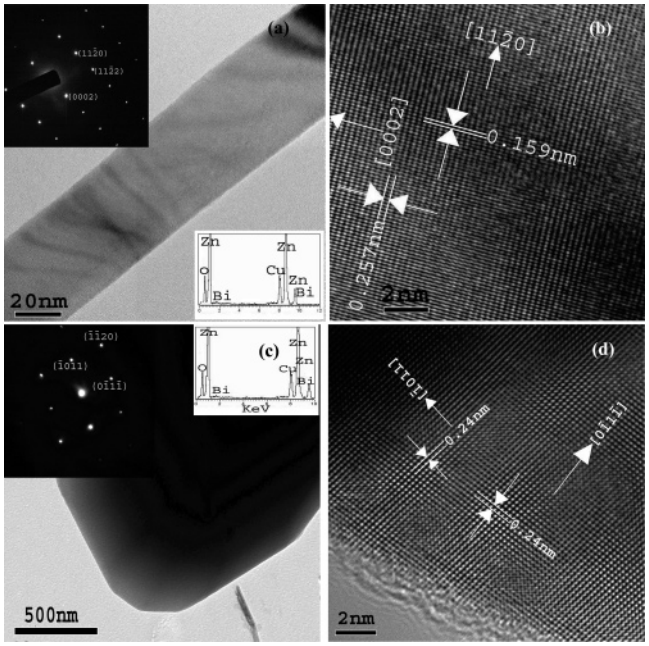

Figure 3. (a) TEM image of a ZnO nanowire. The upper inset is the SAED pattern, and the lower inset is the EDX spectrum. (b) HRTEM image of the same nanowire. (c) TEM image of a nanoplate. The insets are its EDX spectrum and SAED pattern. (d) HRTEM image of the same nanoplate.

which (100), (002), and (101) peaks are relatively strong.[11] It may imply that the nanoplates be selectively oriented. Note that the (102) peak is the most intense feature for the ZnO nanoplates, whereas the (101) peak is the strongest for the ZnO nanowires.

Figure 3a shows a TEM image of a single nanowire, which has a diameter of approximately 40 nm. The EDX data for this nanowire (lower inset in Figure 3a) indicates that it consists of Zn, O, and Bi with Zn/O/Bi = 48.74:51.23:0.03 in atomic concentration. The atomic ratio of Zn to Bi is 99.94:0.06. The selected area electron diffraction (SAED) pattern (upper inset) shows diffraction spots corresponding to a single crystal hexagonal wurtzite ZnO structure with a zone axis of [1$\bar{1}$00], and that the nanowire grew along the [11$\bar{2}$0] direction rather than the [0001] growth direction of conventional ZnO nanowires.[4] Although the EDX data indicated the presence of Bi, no secondary phases were evident in the XRD data. Figure 3b

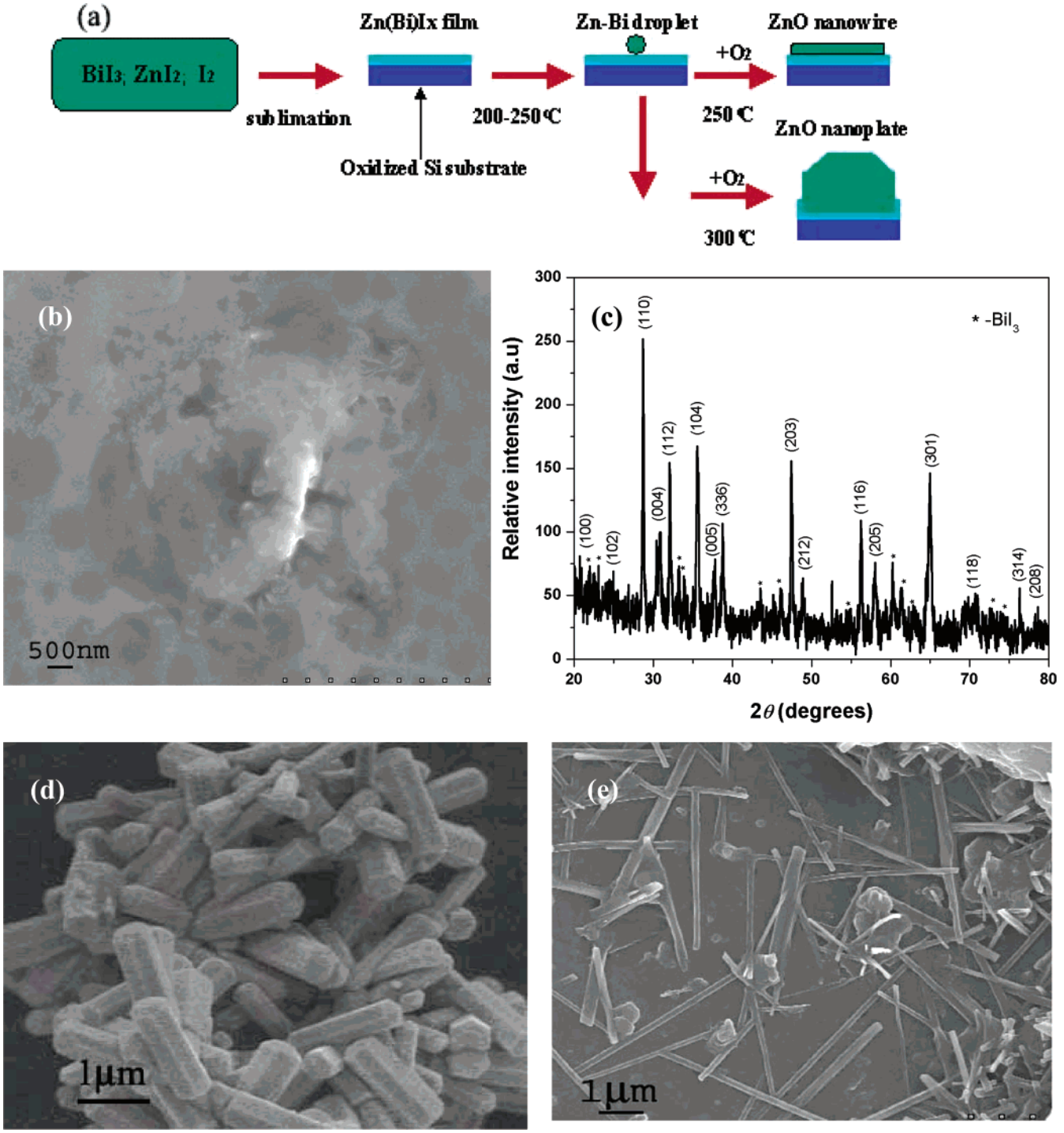

Figure 4. (a) Schematic diagram of the formation mechanism of ZnO nanostructures at 250 and 300 °C. (b) SEM image of the Zn(Bi)I_x thin layer at 250 °C. (c) XRD pattern of the as-obtained layer. The asterisk symbol indicates hexagonal BiI_3. (d) SEM images of ZnO nanorods obtained using Zn and Bi powders as starting materials at 250 °C. (e) SEM images of cogrowth of ZnO nanowires and films at 280 °C.

shows a high-resolution (HR) TEM image of the same nanowire. The interplanar spacings of 0.257 and 0.159 nm correspond to the spacings between (0002) and (11$\bar{2}$0) planes, respectively.

Figure 3c shows a TEM image of an individual nanoplate, which has a thickness of ~40 nm. The EDX results (inset) indicate that the nanoplate consists of Zn, O, and Bi with Zn/O/Bi = 63.36:36.61:0.03 in atomic concentration. The SAED pattern of the nanoplate indicates that it has a single crystal hexagonal wurtzite ZnO structure with a [1$\bar{1}$01] zone axis (a = 3.18 Å, c = 5.18 Å). The nanoplate grew along the [$\bar{1}$011] and [0$\bar{1}\bar{1}$1] directions, rather than the [10$\bar{1}$0] and [01$\bar{1}$0] directions favored by conventional nanodisks.[11] Figure 3d shows a HRTEM image of the same nanoplate. The interplanar spacing of 0.240 nm can be assigned to the spacing between ($\bar{1}$011) planes.

The XRD and TEM data presented above thus indicate that the ZnO nanowires and nanoplates can be achieved by varying temperatures from 250 to 300 °C. Importantly, these data show that the structures of the nanowires and nanoplates prepared in the present work at low temperature differ not only from that of bulk ZnO but also from those of nanostructures with similar shapes grown at high temperature.

To understand the growth mechanism of the nanostructures, a series of experiments were performed. The following mech-

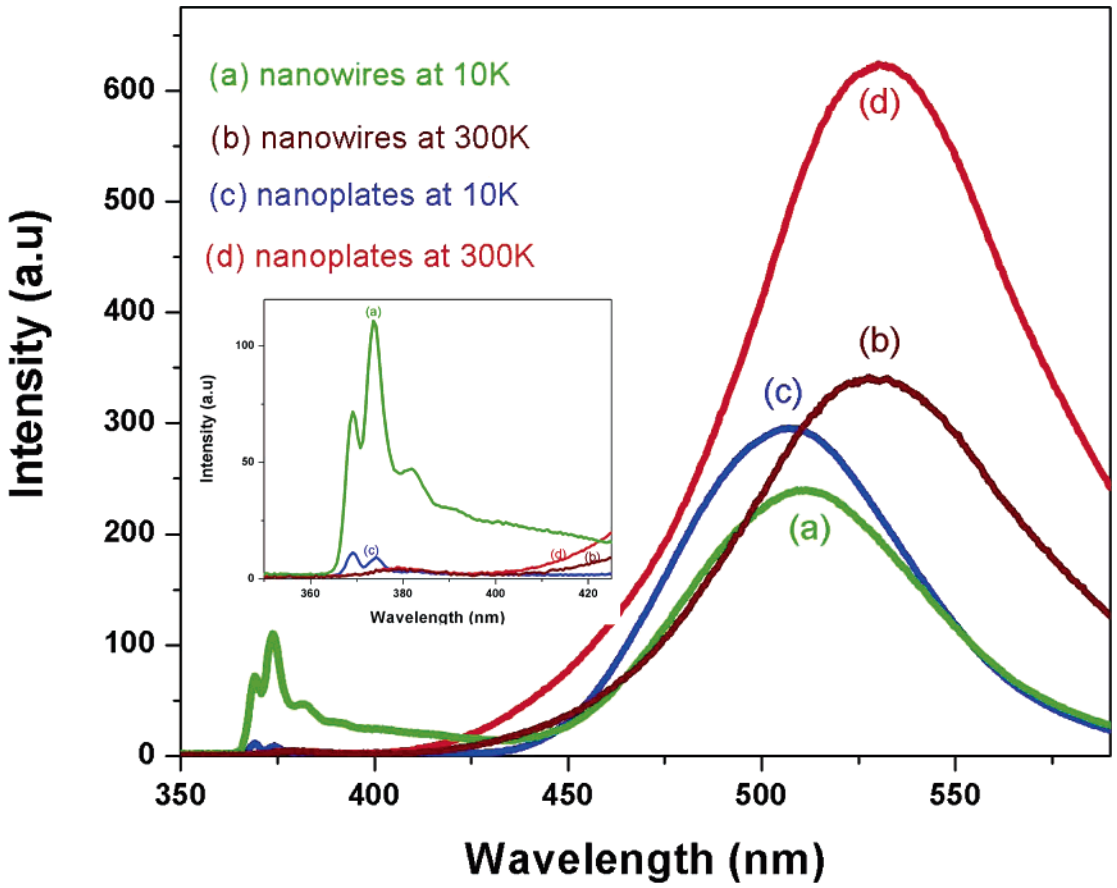

Figure 5. PL spectra of ZnO nanowires and nanoplates at 10 and 300 K. The inset is magnified UV emission of the samples: (a) ZnO nanowires at 10 K; (b) ZnO nanowires at 300 K; (c) ZnO nanoplates at 10 K; (d) ZnO nanoplates at 300 K.

anism, shown schematically in Figure 4a, is proposed on the basis of the experimental results. For the growth of ZnO nanowires, the Zn and BiI_3 first undergo the following reaction at room temperature: $3Zn + 2BiI_3 \leftrightarrow 2Bi + 3ZnI_2$, $2BiI_3 \leftrightarrow 2Bi + 3I_2$, $ZnI_2 \leftrightarrow Zn + I_2$. As the temperature rises from room temperature up to the melting point of the Zn−Bi alloy (~250 °C),[16] ZnI_2, BiI_3 sublime and I_2 are deposited onto the substrate. The observation of a thin layer consisting mainly of Zn and O beneath the nanowires (Figure 1b) provides indirect evidence for this process. More directly, we found that if oxygen was intentionally not introduced during the deposition process, the resulting film had the composition $Zn(Bi)I_x$ (Figure 4b). XRD analysis of this $Zn(Bi)I_x$ film (Figure 4c) indicates that it consists of tetragonal ZnI_2 and hexagonal BiI_3. When the temperature reaches 250 °C, Zn−Bi droplets form, which are vaporized and then deposited on the $Zn(Bi)I_x$ film. Introduction of oxygen into the furnace causes ZnO to nucleate and precipitate from the droplets to form nanowires, because ZnO is not soluble in the droplets. The preference of the ZnO nanowires to grow in the $[11\bar{2}0]$ direction likely arises from the effect of I^- and I_2 on the liquid and the precipitation process. ZnO can be simply described as a number of alternating planes composed of tetrahedrally coordinated O^{2-} and Zn^{2+} ions, stacked alternately along the *c*-axis. The oppositely charged ions produce a spontaneous polarization along the *c*-axis as well as a divergence in surface energies.[17] As both I^- and I_2 are highly polarizable,[13] the sublimation of iodide and/or iodine allows iodine anions and/or iodine molecules to interact with the polar ZnO surface and change the surface energies, suppress or limit the growth direction of nanowires; in other words, iodine and/or iodide have the function of direction conducting for the ZnO nanostructures, resulting in the formation of ZnO nanowires.

We found that if a Zn/Bi mixture was used instead of Zn/BiI_3 as the starting material under the same experimental conditions, no thin layer was observed beneath the nanorods, and the obtained nanorods had typical radial hexagonal cross sections and grew along the [0001] direction (Figure 4d). If Zn or ZnI_2 was used instead of Zn/BiI_3, no nanowires were observed, much less the nanowires with the $[11\bar{2}0]$ direction. From the above results, one can see that no nanowires with the $[11\bar{2}0]$ direction were achieved in the absence of either bismuth or iodine. These findings support the hypothesis that when a Zn/BiI_3 mixture is used as the starting material, the dissociate Bi acts as catalyst and I^- and/or I_2 direct the growth of the ZnO nanowires along the $[11\bar{2}0]$ direction. That is, the growth of ZnO nanowires is dominated by the synergy of vapor−liquid−solid (VLS) and direction conducting from iodide or iodine.

For the growth of ZnO nanoplates, higher density of I^- and/or I_2 arising from the sublimation of iodine and iodide at a relatively high temperature of 300 °C allows strong interaction between I^-/I_2 and the polar ZnO surface, resulting in the formation of ZnO nanoplates. This offers an explanation for why, by absorbing additives such as citrate ions,[18] phosphate ions,[19] and organic dyes[20] on the (0001) surface of ZnO, the growth along the [0001] direction was suppressed, resulting in the formation of ZnO nanoplates.

To further examine the formation of ZnO nanoplates, we investigated the temperature dependence of the nanostructure morphology in the temperature range 250−300 °C. Figure 4e shows a SEM image of the sample grown at 280 °C. When the growth process proceeds at this temperature, the nanowires and the ZnO film grow together such that the nanowires are embedded in the film. From this observation and the results

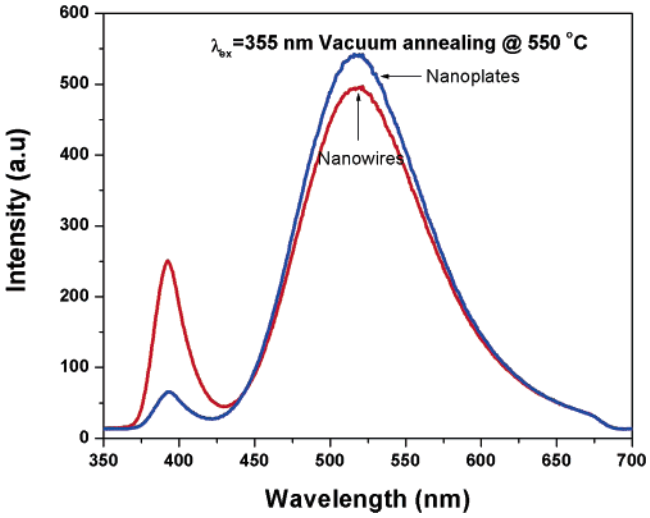

Figure 6. PL spectra of ZnO nanowires and nanoplates after vacuum annealing at 550 °C.

obtained at 250 and 300 °C, we can conclude that at 250 °C the growth rate of the nanowires is faster than that of the film, and hence ZnO nanowires are obtained, whereas at the slightly higher temperature of 280 °C, the growth rate of the film exceeds that of the nanowires. When only ZnI_2 was used as the starting material at 300 °C, a ZnO film was formed but no nanoplates, indicating that the BiI_3 was necessary for the formation of nanoplates. Moreover, experiments in which ZnI_2/BiI_3 was used as the starting material at 300 °C, but the base vacuum was reduced from 300 to 95 mTorr, yielded no nanoplates but a large quantity of nanowires, similar to those obtained at 250 °C with 300 mTorr (at 250 and 280 °C with 95 mTorr, the nanowires were also obtained, SEM based EDX indicated that the nanowires contained I besides Zn and O). These results indicate that, at a relatively low base vacuum of 300 mTorr, the amount of residual oxygen inside the quartz tube plays a role in the initial formation of ZnO nanowires at the relatively low temperature of 250 °C. When the temperature is increased to 280 °C, the nanowires still form but are embedded in the ZnO film due to the faster film growth at higher temperature, indicating that the formation of ZnO nanostructures is in association with not only Bi and I but also temperature, base vacuum (residual oxygen), and pressure.

Figure 5 shows the PL spectra of the ZnO nanowires and nanoplates at 10 and 300 K under the femtosecond optical parametric oscillator (OPO) fourth harmonic at 300 nm of the Ti:sapphire laser (1 MHz, 90 μmW).[21] The inset is the magnified UV emission of the samples. The 10 K PL spectrum of the ZnO nanowires shows narrow UV emissions at 368 and 373 nm as well as a stronger broad green emission band around 510 nm. The intensity ratio of green emission to UV emission (I_G/I_{UV}) is ~2. At 300 K, the broad green emission band is centered at 528 nm, and no UV emission is observed. The 10 K PL spectrum of the ZnO nanoplates exhibits narrow and weak UV emissions at 369 and 374 nm as well as a stronger broad green emission band around 507 nm. The intensity ratio of green emission to UV emission (I_G/I_{UV}) is 21. At 300 K, only the broad green emission band is observed, centered at 530 nm. Thus, increasing the temperature from 10 to 300 K causes a redshift in the green emission band of ~18 nm for the ZnO nanowires and ~23 nm for the ZnO nanoplates. However, this band is more intense at 300 K than at 10 K for both the nanowires and nanoplates. The UV emission peaks are closely related to the radiative annihilation of excitons,[22] and the green emission can be assigned to oxygen vacancy.[15,23] The redshift of green emission on going from 10 to 300 K can thus be mainly attributed to oxygen vacancies and/or defects in the ZnO nanostructures. Moreover, the observation of a larger redshift for the ZnO nanoplates compared to the ZnO nanowires suggests that the former contain higher concentrations of oxygen vacancies and/or defects. The intensity ratio of green emission to UV emission (I_G/I_{UV}) is related to the surface area ratio. Thus, the much higher value of I_G/I_{UV} for the ZnO nanoplates compared to the ZnO nanowires ($I_G/I_{UV} = 21$ and 2, respectively) at 10 K indicates that the nanoplates have higher surface-to-volume ratios than the nanowires. Figure 6 shows the room-temperature PL spectra of ZnO nanowires and nanoplates after vacuum annealing at 550 °C for 1 h, under the third harmonic at 355 nm of a Nd:YAG laser (13 kHz, 10 mW). As seen from the spectra, the UV emissions of nanowires and nanoplates are visible. The room-temperature UV emissions after vacuum annealing are consistent with the involvement of oxygen vacancies.[24,25] I_G/I_{UV} of ZnO nanoplates (~8) is higher than that of nanowires (~2), further indicating that the nanoplates contain more oxygen vacancies than nanowires.

4. Conclusions

In summary, starting from a mixture of Zn and BiI_3, we grew nanowires and nanoplates on an oxidized Si substrate at relatively low temperatures of 250 and 300 °C, respectively. The ZnO nanowires had diameters of ~40 nm and grew along the $[11\bar{2}0]$ direction rather than the conventional [0001] direction. The nanoplates had a thickness of ~40 nm and lateral dimensions of 3−4 μm. The growth of both the nanowires and nanoplates is dominated by the synergy of VLS and direction conducting. Analysis of photoluminescence spectra suggested that the nanoplates contain more oxygen vacancies and have higher surface-to-volume ratios than the nanowires. The present results clearly demonstrate that the shapes of ZnO nanostructures formed by using BiI_3 can be controlled by varying the temperature in the range 250−300 °C.

Acknowledgment. This work was partially supported from electron Spin Science Center (eSSC), National Research Laboratory (NRL) projects which are funded by Korean Science and Engineering Foundation (KOSEF) and Brain Korea (BK) 21.

References and Notes

(1) Park, W. I.; Kim, D. H.; Jung, S. W.; Yi, G. C. *Appl. Phys. Lett.* **2002**, *80*, 4232.
(2) Li, Y. B.; Bando, Y.; Sato, Y. T. Kurashima, K. *Appl. Phys. Lett.* **2002**, *81*, 144.
(3) Wang, X.; Li, Q.; Liu, Z.; Zhang, J.; Z. Liu, Z. *Appl. Phys. Lett.* **2004**, *84*, 4941.
(4) Xu, C. K.; Xu, G. D.; Liu, Y. K.; Wang, G. H. *Solid State Commun.* **2002**, *122*, 175.
(5) Xu, C. K.; Rho, K.; Chun, J.; Kim, D. E. *Appl. Phys. Lett.* **2005**, *87*, 253104.
(6) Yang, B.; Wu, Y.; Zong, B.; Shen, Z. *Nano Lett.* **2002**, *2*, 751.
(7) Monge, M.; Kahn, M. L.; Maisonnat, A.; Chaudret, B. *Angew. Chem., Int. Ed.* **2003**, *42*, 5321.
(8) Ghezelbash, A.; Sigman, M. B., Jr.; Korgel, B. A., Jr. *Nano Lett.* **2004**, *4*, 537.
(9) Puntes, V. F.; Zanchet, D.; Erdonmez, C. K.; Alivisatos, A. P. *J. Am. Chem. Soc.* **2002**, *124*, 12874.
(10) (a) Cao, Y. C. *J. Am. Chem. Soc.* **2004**, *126*, 7456. (b) Cao, B.; Cai, W.; Li, Y.; Sun, F.; Zhang, L. *Nanotechnology* **2005**, *16*, 1734.
(11) Xu, C. X.; Sun, X. W.; Dong, Z. L.; Yu, M. B. *Appl. Phys. Lett.* **2004**, *85*, 3878.
(12) Tyagi, P.; Vedeshwar, A. G. *Phys. Rev. B* **2001**, *64*, 245406.
(13) Song, Y.; Niu, Y.; Hou, H.; Zhu, Y. *J. Mol. Struct.* **2004**, *689*, 69.
(14) Xu, C. K.; Rho, K.; Chun, J.; Kim, D. E. *Nanotechnology* **2006**, *17*, 60.
(15) Xu, C. K.; Kim, M.; Chun, J.; Kim, D. E. *Nanotechnology* **2005**, *16*, 2104.

(16) Yumato, H.; Kaneko, Hasiguti, T. R. R.; Watanabe, T. *J. Cryst. Growth* **1987**, *84*, 185.
(17) Wang, Z. L.; Kong, X. Y.; Ding, Y.; Gao, P.; Hughes, W.; Yang, R.; Zhang, Y. *Adv. Funct. Mater.* **2004**, *14*, 904.
(18) Tian, Z. R.; Voigt, J. A.; Liu, J.; Mckenzie, B.; Mcdermott, M. J. *J. Am. Chem. Soc.* **2002**, *124*, 12954.
(19) Imai, H.; Iwai, S.; Yamabi, S. *Chem. Lett.* **2004**, *33*, 768.
(20) Yoshida, T.; Tochimoto, M.; Schlettwein, D.; Wohrle, D.; Sugiura, T.; Minoura, H. *Chem. Mater.* **1999**, *11*, 2657.
(21) Min, C. K.; Joo. T. *Opt. Lett.* **2005**, *30*, 1855.
(22) Wu, J. J.; Wen, H. I.; Tseng, C. H.; Liu, S. C. *Adv. Funct. Mater*. **2004**, *14*, 806.
(23) Kong, Y. C.; Yu, D. P.; Zhang, B.; Fang, W.; Feng, S. Q. *Appl. Phys. Lett.* **2001**, *78*, 407.
(24) Wang, D.; Seo, H. W.; Tin, C. C.; Bozack, M. J.; Williams, J. R.; Park, M.; Sathitsuksanoh, N.; Cheng, A. J.; Tzeng, Y. H. *J. Appl. Phys.* **2006**, *99*, 113509.
(25) Greene, L. E.; Law, M.; Goldberger, J.; Kim, F.; Johnson, J. C.; Zhang, Y.; Saykally, R. J.; Yang, P. *Angew. Chem., Int. Ed.* **2003**, *42*, 3031.